phys. stat. sol. (c) **2**, No. 7, 2928–2931 (2005) / **DOI** 10.1002/pssc.200461289

Modelling study of MQW LED operation

V. F. Mymrin[1], **K. A. Bulashevich**[1], **N. I. Podolskaya**[1], **I. A. Zhmakin**[1], **S. Yu. Karpov**[*1], and **Yu. N. Makarov**[2]

[1] Soft-Impact, Ltd., P.O.Box 83, 27 Engels av., St. Petersburg 194156, Russia
[2] Semiconductor Technology Research, Inc., P.O. Box 70604, Richmond, VA, 23255-0604, USA

Received 21 June 2004, revised 18 October 2004, accepted 18 October 2004

PACS 78.60.Fi, 85.60.Bt, 85.60.Jb

Operation of multiple-quantum-well (MQW) light emitting diode (LED) heterostructures with selective barrier doping is studied by modelling. The carrier confinement in the MQW LEDs and the effects of barrier doping on the emission efficiency and wavelength stability is examined in detail. The simulations predict improvement of the LED performance by heavy n-doping of the MWQ barriers. The theoretical predictions are compared with available experimental data.

1 Introduction

Enormous growth of III-nitride-based light emitting diode market observed in the last years demands a careful optimization of both fabrication technology and design of these devices. Much effort has been made to improve the material quality [1, 2], efficiency of light extraction from LEDs [3, 4], and contact geometry [4]. However, much less studies dealing with optimization of LED heterostructures are reported to date. In particular, this concerns a choice between a single-quantum-well (SQW) and multiple-quantum-well active region in LEDs. Despite the reported advantages of using SQW active regions [5], the potentiality of MQW ones, in our opinion, is not yet exhausted and require more detailed examination.

The modelling study reported in this paper is aimed at better understanding the operation of MQW LED heterostructures with the focus on the carrier confinement in the active region and the role of selective doping in the barriers separating individual quantum wells. This research was stimulated by the reported improvement of the LED efficiency and wavelength stability due to the use of the enhanced barrier doping [4,6].

2 Results and discussion

Blue MQW LED heterostructure similar to those examined in [4,6] has been chosen for simulations. The Ga-faced structure consists of the GaN:Si contact layer ([Si] = 2×10^{18} cm^{-3}), the MQW active region, the $Al_{0.15}Ga_{0.85}N$:Mg emitter ([Mg] = 1.5×10^{19} cm^{-3}) 60 nm thick, and the GaN:Mg contact layer ([Mg] = 2×10^{19} cm^{-3}). The active region contains four undoped (as assumed) $In_{0.13}Ga_{0.87}N$ quantum wells (QWs) 3 nm thick separated by the GaN:Si barriers 12 nm thick. Every barrier is doped with the Si concentration varied between 5×10^{17} cm^{-3} and 5×10^{18} cm^{-3}. All the epilayers are considered to be grown coherently on the thick GaN:Si contact layer, i.e. no strain relaxation is assumed to occur in the material.

To simulate the MQW LED operation, we used the package SiLENSe [7] implementing the 1D model based on the Poisson equation for the electric potential and drift-diffusion transport equations for the

---

[*] Corresponding author: e-mail: karpov@softimpact.ru, Phone: +7 812 554 4570, Fax: +7 812 326 6194

electron and hole concentrations. Both the radiative recombination of the carriers and their non-radiative recombination on threading dislocation cores [8] are considered to predict the internal light emission efficiency of the LEDs. The Fermi-Dirac statistics is used, accounting for high non-equilibrium electron and hole concentrations in the active region. To calculate the light emission spectra, we solve self-consistently the Poisson and Schrödinger equations for the carrier wave functions inside each quantum well. A uniform spectra broadening, $\Gamma = 20$ meV, due to momentum relaxation via electron-electron collisions is accounted for in simulations. The complex valence band structure of nitride semiconductors is allowed for within the Luttinger-Kohn approach [9]. All the computations discussed below have been carried out with the threading dislocation density of 10^8 cm^{-2}. This value is by the order of magnitude lower than the dislocation density typical to MOCVD-grown heterostructures, which accounts for the suppression of the dislocation-mediated non-radiative carrier recombination due to fluctuations of In composition in the MQWs [10].

Fig.1 shows the band diagrams and distributions of carrier concentrations in the LED structure with [Si] = 5×10^{18} cm^{-3} in the barriers, computed for two practically important values of current density j. It is seen that in the whole range of current density variation, electrons are uniformly distributed over different QWs. In contrast, holes are injected mainly into the QW adjacent to the p-AlGaN emitter at a lower j, while they fill the rest QWs at j exceeding 100-200 A/cm^2. The hole distribution over the QWs becomes much more uniform if the lightly doped barriers ([Si] = 5×10^{17} cm^{-3}) are employed in the LED structure. This is due to a lower carrier recombination rate (a higher diffusion length) in the active region directly controlled by the electron concentration.

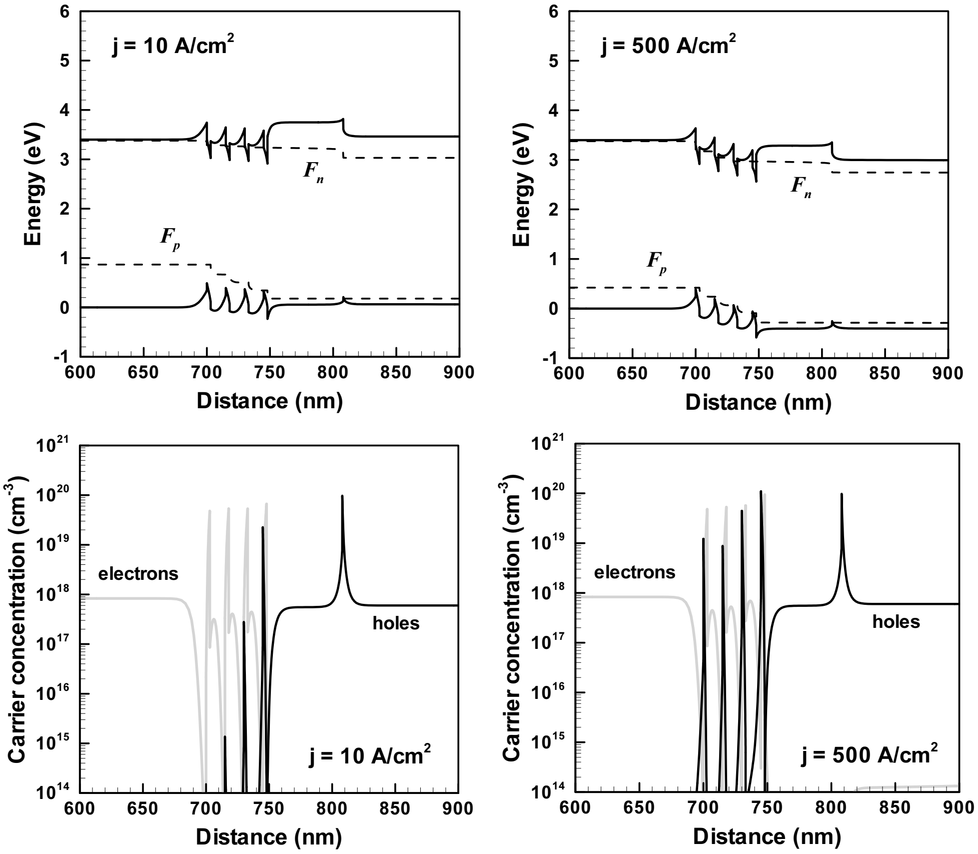

Fig. 1 Band diagrams and distributions of carrier concentrations in the MQW LED with [Si] = 5×10^{18} cm^{-3} in the barriers. The quasi-Fermi levels of electrons and holes are denoted as F_n and F_p , respectively.

The radiative recombination of electrons and holes is found to be localized mainly in the QWs. The non-radiative recombination occurs also in the MQW barriers and p-GaN contact layer where mobile electrons can penetrate to. The latter effect is caused by insufficiently high potential barrier in the p-AlGaN emitter which fails to confine electrons at high current densities (see Fig. 1).

The I-V characteristic of the MQW LED computed for the serial resistance of $R_S = 7\ \Omega$ is compared with that measured on the sample b026 in [6] (Fig. 2). Excellent agreement is seen except for the low-current region where the tunnelling current is believed to dominate, which is not allowed for in the computational model. It is seen from the comparison that in the practically important range of current density variation, 10-500 A/cm^2, the MQW LED operates in the injection-current mode.

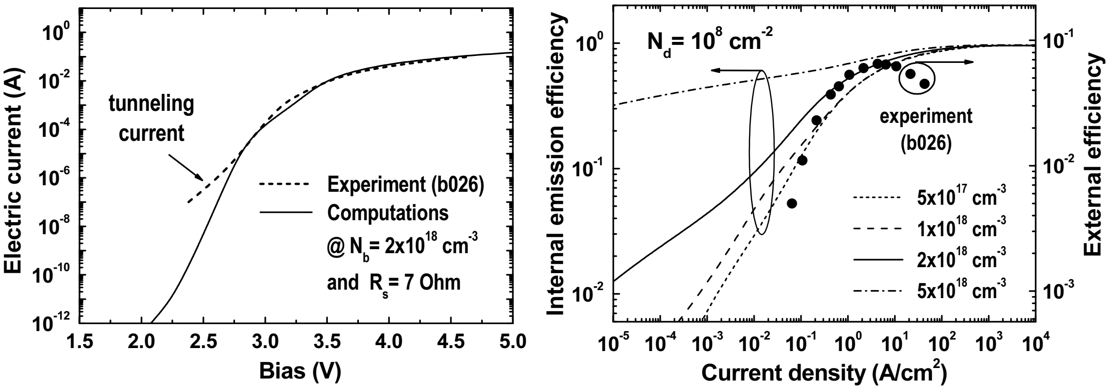

Fig. 2 I-V characteristic (left) and internal emission efficiency *versus* current density (right) computed for various donor concentrations in the barriers. Circles (right) are the external emission efficiency of an LED measured in [6].

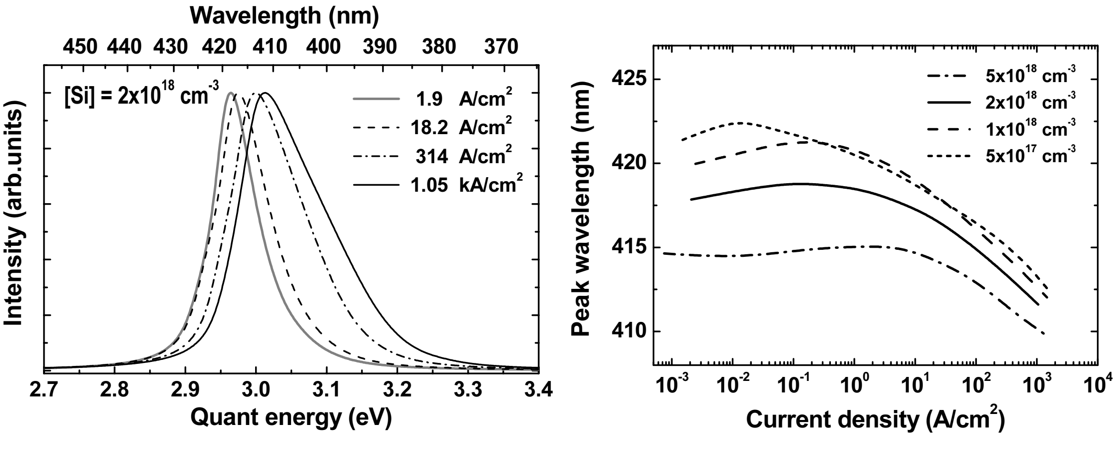

Fig. 3 Emission spectra from the LED structure with [Si] = 2×10^{18} cm^{-3} in the barriers (left) and the peak wavelength as a function of current density computed for various donor concentrations in the barriers (right).

Fig.2 shows the internal emission efficiency (the ratio of the photon emission rate to the rate of electron-hole pair injection in the LED structure) as function of current density computed for various donor concentrations in the MWQ barriers. For comparison, the external efficiency measured in [6] is also plotted in the figure. One can see that the predicted internal and measured external efficiencies correlate with each other and even are in quantitative agreement, if the efficiency of light extraction from the LED and its collection by the measuring system is assumed to be of ~ 11%. The internal efficiency is found to depend drastically on the donor concentration in the MQW barriers, especially at low currents, which is confirmed by the data reported in [6].

Two factors may give rise to the emission efficiency enhancement in a heavily doped LED structure. First, as was shown in [8], a higher overall electron concentration in the material favours suppression of the non-radiative recombination due to a prolonged time of carrier capture on threading dislocation cores. Second, in a heavily doped structure, holes are injected mostly into the QW adjacent to the p-emitter where the radiative recombination dominates (see Fig. 1, left). In contrast, in a lightly doped LED, holes are distributed much more uniformly over all the QWs, passing through the barriers where the non-radiative carrier recombination dominates. Suppression of the non-radiative recombination in the barriers due to a non-uniform hole distribution may be an additional factor contributing to the emission efficiency at a higher doping level in the MQW barriers.

Additional reason for the use of heavily doped MQW barriers was the observed enhancement of the emission wavelength stability of the LED [6]. Our simulations confirm that a higher barrier doping results in better peak wavelength stability at $j \le 10$ A/cm^2 (Fig. 3). At higher current densities, however, a distinct blue shift is predicted for all the structures irrespective of the barrier doping. Typical emission spectra computed for various injection levels are plotted in Fig. 3, left. The electroluminescence peak becomes broadened at high current densities, which is due to the contribution of higher electron subbands in the radiative recombination. Both heavy and light holes form a quasi-continuum of states in the quantum wells, which is not resolved in the emission spectra. The predicted peak energy is found to be shifted from the experimental values by ~0.3 eV. This discrepancy may be attributed to either additional doping of the quantum wells with acceptors [11] or poorly known InGaN QW composition. In any case, this uncertainty does not affect the injection properties and general behavior of the LED structure discussed above.

3 Conclusion

In this paper, we report on the modelling study of a MQW LED heterostructure with selectively doped barriers. The device operates in the injection-current mode in the practically important range of current density variation, which is derived from the comparison of the computed and measured I-V characteristics of the LED. The simulations predict efficient capture of injected holes by the QWs and insufficient confinement of electrons by the p-AlGaN emitter barrier at high current densities j. Heavy MQW barrier doping with donors is found to enhance the internal emission efficiency of the device and to stabilize the emission wavelength at moderate current densities $j \le 10$ A/cm^2. These predictions agree well with observations reported in Refs. [4, 6]. At higher current densities, the spectra exhibit a distinct blue shift and broadening due to filling of higher electron subbands.

References

[1] T. Mukai, S. Nagahama, M. Sano, T. Yanamoto, D. Morita, T. Mitani, Y. Narukawa, S. Yamamoto, I. Niki, M. Yamada, S. Sonobe, S. Shioji, K. Deguchi, T. Naitou, H. Tamaki, Y. Murazaki, and M. Kameshima, phys. stat. sol. (a) **200**, 52 (2003).

[2] S. Kamiyama, M. Iwaya, H. Amano, and I. Akasaki, phys. stat. sol. (a) **194**, 393 (2002).

[3] J. Baur, B. Hahn, M. Fehrer, D. Eisert, W. Stein, A. Plössl, F. Kühn, H. Zull, M. Winter, and V. Härle, phys. stat. sol. (a) **194**, 399 (2002).

[4] A. Y. Kim, W. Götz, D. A. Steigerwald, J. J. Wierer, N. F. Gardner, J. Sun, S. A. Stockman, P. S. Martin, M. R. Kramers, R. S. Kern, and F. M. Steranka, phys. stat. sol. (a) **188**, 15 (2001).

[5] M. Koike, N. Shibata, S. Yamasaki, S. Nagai, S. Asami, H, Kato, N, Koide, H. Amano, and I. Akasaki, Mat. Res. Soc. Symp. Proc. **395**, 889 (1996).

[6] S. S. Mamakin, A. E. Yunovich, A. B. Wattana, and F. I. Manyakhin, Semiconductors **37**, 1107 (2003).

[7] http://www.semitech.us/products/SiLENSe/

[8] S.Yu. Karpov and Yu.N. Makarov, Appl. Phys. Lett. **81**, 4721 (2002).

[9] S.-H. Park and S.-L. Chuang, J. Appl. Phys. **87**, 353 (2000).

[10] S. Yu. Karpov, K. A. Bulashevich, I. A. Zhmakin, M. O. Nestoklon, V. F. Mymrin, and Yu. N. Makarov, phys. stat. sol. (b) **241**, 2668 (2004).

[11] S. Nakamura, J. Vac. Sci. Technol. A **13**, 705 (1995).